Journal of ELECTRONIC MATERIALS, Vol. 38, No. 7, 2009
DOI: 10.1007/s11664-008-0654-6

Thermoelectric Characterization of $(Ga,In)_2Te_3$ with Self-Assembled Two-Dimensional Vacancy Planes

S. YAMANAKA,[1] M. ISHIMARU,[2] A. CHAROENPHAKDEE,[1] H. MATSUMOTO,[1] and K. KUROSAKI[1,3]

1.—Graduate School of Engineering, Osaka University, Suita, Osaka 565-0871, Japan. 2.—Institute of Scientific and Industrial Research, Osaka University, Ibaraki, Osaka 567-0047, Japan. 3.—e-mail: kurosaki@see.eng.osaka-u.ac.jp

The key properties for the design of high-efficiency thermoelectric materials are a low thermal conductivity and a large Seebeck coefficient with moderate electrical conductivity. Recent developments in nanotechnology and nanoscience are leading to breakthroughs in the field of thermoelectrics. The goal is to create a situation where phonon pathways are disrupted due to nanostructures in "bulk" materials. Here we introduce promising materials: $(Ga,In)_2Te_3$ with unexpectedly low thermal conductivity, in which certain kinds of superlattice structures naturally form. Two-dimensional vacancy planes with approximately 3.5-nm intervals exist in Ga_2Te_3, scattering phonons efficiently and leading to a very low thermal conductivity.

Key words: Thermoelectrics, thermal conductivity, nanostructured materials, gallium telluride, indium telluride

INTRODUCTION

Thermoelectric technology, which can convert waste heat into useful electricity, is expected to play an important role in meeting today's energy challenges.[1] The efficiency of the device is linked to the thermoelectric properties of the generator materials and the temperature gradient across the device. The effectiveness of the thermoelectric materials is determined by the dimensionless thermoelectric figure of merit, $ZT = S^2\sigma T/\kappa$, where S, σ, T, and κ are, respectively, the Seebeck coefficient, electrical conductivity, absolute temperature, and thermal conductivity. The most important issue in thermoelectric research is identifying materials with high ZT, namely with low κ as well as large S with moderate σ. Recently, low-κ semiconductors and/or semimetals such as Zn_4Sb_3[2] filled skutterudites,[3] and Ag_9TlTe_5[4] have been proposed as next-generation advanced thermoelectric materials.

(Received August 1, 2008; accepted December 30, 2008; published online January 24, 2009)

The best thermoelectric materials currently used in devices are Bi_2Te_3-based alloys with a maximum ZT of around 1. $ZT \approx 1$, which translates to a device efficiency of several percent, was a practical upper limit for bulk materials established in the 1960s. In developing a thermoelectric power generator for the consumer market, such as the automotive industry, a key factor is the achievement of a device efficiency of at least 20%, corresponding to $ZT \approx 2$ or more.

Since the S, σ, and κ in bulk materials are interrelated, it is very difficult to control them independently so that ZT can be increased. However, the assumption is that, if numerous nanoscale interfaces are introduced, the interfaces would scatter phonons more efficiently than electrons, leading to significant reduction of κ without prejudice to S and σ.[5–7] There have been a few previous studies aimed at establishing proof of principle of this concept. For example, Venkatasubramanian et al.[8] and Harman et al.[9] performed thermoelectric characterizations on Bi_2Te_3/Sb_2Te_3 superlattices and PdTe/PdSeTe quantum-dot superlattices, respectively. They demonstrated that the scattering of phonons by the interfaces reduced

the κ more than the σ, leading to the achievement of $ZT > 2$. While ZT has reached high values in such superlattice structures, these materials are unlikely candidates for practical use. The goal is to achieve similarly high ZT in "bulk" materials that can be developed in large quantities with lower manufacturing complexity and cost. Hsu et al.[10] reported the exceptionally high ZT (>2) of PbTe-based bulk materials due to the very low κ, possibly arising from the compositional modulations on the single-nanometer scale, similar to that found in superlattices. However, this is just one way to realize high ZT with bulk-nanostructured materials.

Against this background, we focused attention on semiconductor $(Ga,In)_2Te_3$ as examples of bulk-nanostructured materials. It is well known that Ga_2Te_3 and In_2Te_3 have the same crystal structure: a defect zincblende cubic crystal (space group F-43m). Due to the valence mismatch between the cation and anion, one-third of the cation sites are structural vacancies in both Ga_2Te_3 and In_2Te_3; i.e., the chemical formula of M_2Te_3 (M = Ga and In) can be described as $M_2VA_1Te_3$, where VA means vacancy. However, the vacancy distribution is different in Ga_2Te_3 and In_2Te_3. Desai et al. demonstrated that In_2Te_3 has two components, a low-temperature α-phase with regularly ordered vacancies and a high-temperature β-phase with fully disordered vacancies; the former transforms to the latter at about 893 K.[11] α-In_2Te_3 has a face-centered cubic lattice with a = 1.850 nm, which is approximately three times the lattice parameter of β-In_2Te_3 (a = 0.616 nm). On the other hand, it has been observed that Ga_2Te_3 has a mesoscopic superstructured phase, having periodic vacancy planes,[12,13] as observed in Ga_2Se_3.[14] We hypothesized that, if we could create such vacancy planes in the bulk samples and control their size and periodicity, we could achieve a low κ, due to the effective phonon scattering by the vacancy planes. In the present study, therefore, we performed thermoelectric characterizations of $(Ga,In)_2Te_3$, and tried to control the formation of the vacancy planes. We studied the relationship between the thermoelectric properties (especially κ) and the periodicity of the vacancy-plane intervals.

EXPERIMENTAL PROCEDURE

We prepared five compositions of the samples $(Ga_{1-x}In_x)_2Te_3$ (x = 0, 0.25, 0.5, 0.75, and 1). Appropriate amounts of Ga_2Te_3 and In_2Te_3 were sealed in silica tubes and melted at 1273 K overnight, then annealed at 973 K for 2 weeks, followed by quenching. We can get the raw materials, Ga_2Te_3 and In_2Te_3 chunks, from some Japanese chemical companies. To obtain fully dense polycrystalline samples for characterizations, the obtained ingots were crushed to fine powders followed by hot-pressing at 873 K for 3 h under a pressure of 62 MPa in an argon flow atmosphere.

To characterize the crystallographic properties of the samples, we collected powder x-ray diffraction (XRD) data on a diffractometer (RINT2000, RIGAKU) with Cu Kα radiation in air at room temperature. The sample density was calculated from the sample size and weight at room temperature.

The thermal conductivity (κ) was calculated from the heat capacity (C_P), thermal diffusivity (α), and density (d) using the relationship $\kappa = \alpha C_P d$. The heat capacity was estimated from the model of Dulong and Petit, that is, $C_P = 3nR$, where n is the number of atoms/f.u. and R is the gas constant. The thermal diffusivity was measured by the laser flash method using TC-7000 (ULVAC) in a vacuum. Electrical resistivity (ρ) and the Seebeck coefficient (S) were measured by using ZEM apparatus (ULVAC) in a helium atmosphere, in which ρ was measured by a DC four-probe technique.

Transmission electron microscopy (TEM) observations were performed using a JEOL JEM-3000F with an incident electron energy of 300 keV. Flakes of single crystals, obtained by crushing the pellets, were used for TEM samples. High-resolution TEM images and electron diffraction patterns were recorded on imaging plates.

RESULTS AND DISCUSSION

Figure 1 shows the powder x-ray diffraction (XRD) patterns of polycrystalline $(Ga_{1-x}In_x)_2Te_3$ (x = 0, 0.25, 0.5, 0.75, and 1) samples prepared in

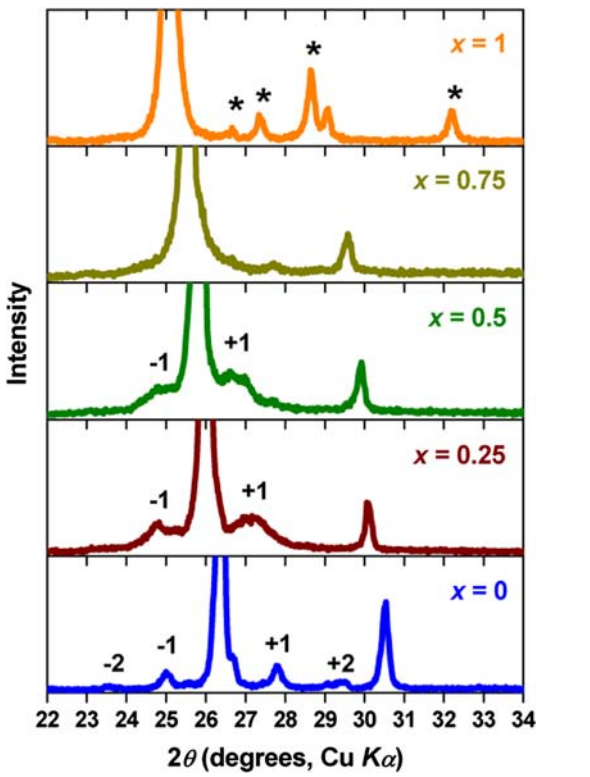

Fig. 1. Powder XRD patterns of $(Ga_{1-x}In_x)_2Te_3$ (x = 0, 0.25, 0.5, 0.75, and 1).

the present study. Basically, all the peaks could be indexed as having the zincblende structure. In_2Te_3 can be indexed as $3 \times 3 \times 3$ of the zincblende unit cell, which was well consistent with the reported crystal structure of α-In_2Te_3.[15] Peaks derived from the ordered-vacancy distribution in the In_2Te_3 crystal are denoted by asterisks. Peaks corresponding to the zincblende structure shift to lower angle with increasing x in $(Ga_{1-x}In_x)_2Te_3$, indicating that the lattice parameter increases with x. On the other hand, in the XRD patterns of $(Ga_{1-x}In_x)_2Te_3$ (x = 0, 0.25, and 0.5), a few peaks were observed before and after the (111) peak, suggesting that the vacancy may concentrate on the (111) plane. In addition, these satellite peaks broaden with x. This peak broadening is closely related with the periodicity of the vacancy-plane intervals, as described in the next section. Perhaps, in the x = 0.75 sample, the satellite peaks are too broad to be detected or the positions are behind the (111) peak.

Figure 2 shows high-resolution TEM images and electron diffraction patterns taken from a single grain of a sintered pellet of $(Ga_{1-x}In_x)_2Te_3$ (x = 0, 0.25, 0.5, 0.75, and 1). These micrographs were obtained with the electron beam aligned along the $[1\bar{1}0]$ direction. In the electron diffraction pattern of Ga_2Te_3, superlattice spots exist at the ~1/10 positions between two neighboring fundamental spots along the [111] direction, in addition to the fundamental Bragg reflections due to the zincblende structure. In the high-resolution TEM image of Ga_2Te_3, plane defects due to the vacancy-rich plane are two-dimensionally arranged throughout the whole area of the sample. These plane defects appear at the (111) plane with approximately 10-lattice (equivalent to 3.5 nm) intervals, consistent with the electron diffraction pattern. On the other hand, In_2Te_3 possesses a triple periodicity along the [111] direction, as shown in the high-resolution TEM image, well consistent with the electron diffraction pattern, in which the superlattice spots exist at the 1/3 positions. In the high-resolution TEM images of $(Ga_{1-x}In_x)_2Te_3$ (x = 0.25, 0.5, and 0.75), there exist two-dimensional vacancy planes at the (111) plane like Ga_2Te_3, however the periodicity of the interval is random. In particular, the vacancy planes appear with approximately 3–15 lattice intervals in the solid-solution samples. These TEM results are well consistent with both the electron diffraction and the XRD patterns. In the electron diffraction patterns, the superlattice reflections are diffuse and a streak can be seen. And also, it can be seen a broadening of the satellite peaks in the XRD pattern (Fig. 1), which is most likely caused by the random periodicity of the vacancy-plane intervals.

Figure 3 shows the temperature dependence of the thermal conductivities of $(Ga_{1-x}In_x)_2Te_3$ (x = 0, 0.25, 0.5, 0.75, and 1). The molecular weight of In_2Te_3 (612.4) is heavier than that of Ga_2Te_3 (522.24), and as expected, the Debye temperature (θ) of α-In_2Te_3 (159 K) was lower than that of Ga_2Te_3 (245 K). So, we predicted a lower κ for In_2Te_3 than for Ga_2Te_3; however, we got the opposite result. The κ of Ga_2Te_3 is lower than that of In_2Te_3 in the whole temperature range, and the values are unexpectedly low, around 0.5 W m^{-1} K^{-1}. This indicates the possible presence of highly effective phonon scattering in Ga_2Te_3, which is due to the two-dimensional vacancy-plane structures. The solid solutions, especially the samples with

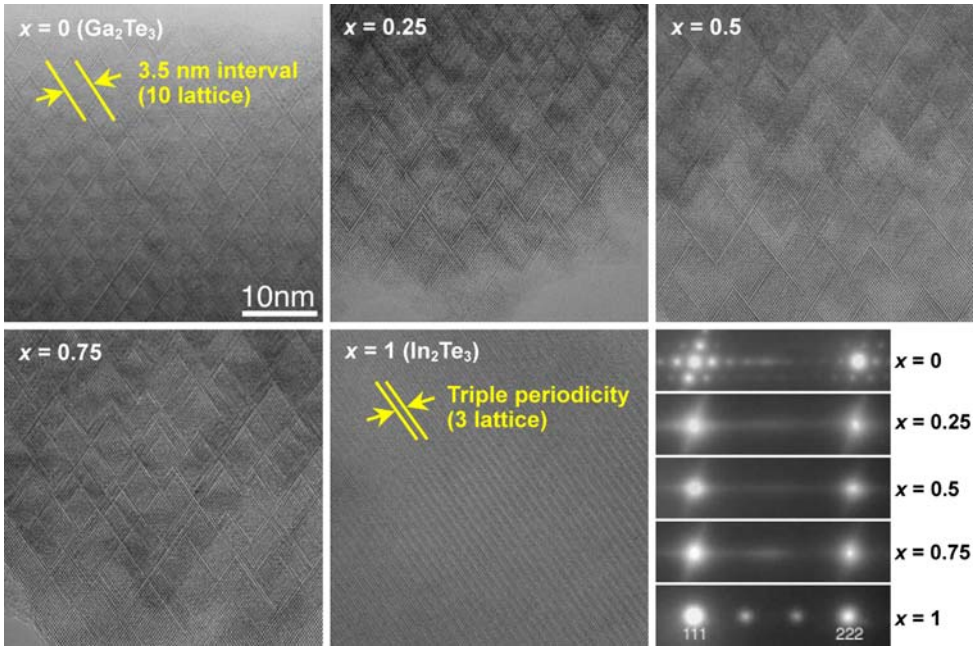

Fig. 2. High-resolution TEM images and electron diffraction patterns taken from a single grain of the sintered pellet of $(Ga_{1-x}In_x)_2Te_3$ (x = 0, 0.25, 0.5, 0.75, and 1) obtained with the electron beam aligned along the $[1\bar{1}0]$ direction.

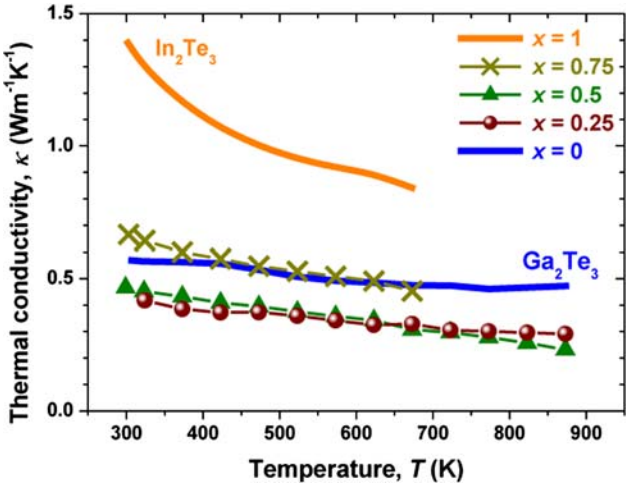

Fig. 3. Temperature dependence of the thermal conductivity (κ) of $(Ga_{1-x}In_x)_2Te_3$ (x = 0, 0.25, 0.5, 0.75, and 1).

compositions of x = 0.25 and 0.5, indicate very low κ of 0.25 W m^{-1} K^{-1} to 0.5 W m^{-1} K^{-1}, even lower than that of Ga_2Te_3. This low κ of the solid solutions would be primarily due to both alloying effect between Ga and In and the random periodicity of the vacancy-plane intervals.

Figure 4 shows the temperature dependence of the electrical resistivity (ρ), Seebeck coefficient (S), and power factor (S^2/ρ) of $(Ga_{1-x}In_x)_2Te_3$ (x = 0, 0.25, 0.5, 0.75, and 1). The S of all samples show large positive values and a negative temperature dependence, whereas the ρ has relatively high values and a negative temperature dependence. The ρ systematically increases with x, while there is no clear relationship between the magnitude of S and x. The power factor values of all solid-solution samples are lower than that of Ga_2Te_3. No improvement in the power factor can be achieved in the solid-solution system. Although its electrical performance is not exceptional, Ga_2Te_3 exhibits a relatively high ZT value, approximately 0.16 at 850 K, primarily due to its very low κ. This means that there is further opportunity for improvement of the ZT; viz., the ZT could be enhanced after tuning its carrier concentration.

SUMMARY

In the present study, polycrystalline fully dense samples of $(Ga_{1-x}In_x)_2Te_3$ (x = 0, 0.25, 0.5, 0.75, and 1) were prepared and their thermoelectric properties were characterized. Ga_2Te_3 proved notably interesting since its κ values were unexpectedly low in view of its simple crystal structure. From the atomistic structure observations, we confirmed the existence in Ga_2Te_3 of regularly arranged two-dimensional vacancy planes with approximately 10-lattice (equivalent to 3.5 nm) intervals. In the solid solutions of $(Ga,In_x)_2Te_3$, such vacancy planes also exist, but the periodicity of the intervals is

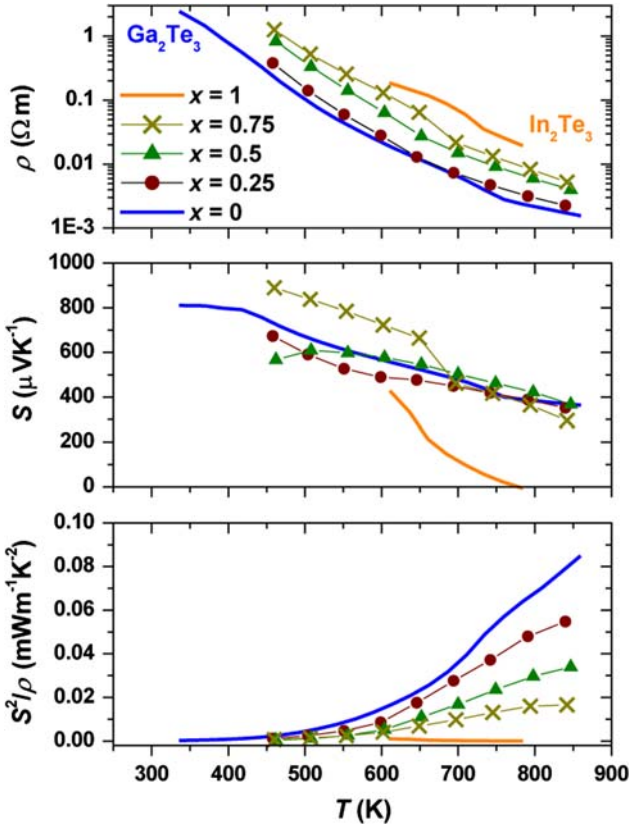

Fig. 4. Temperature dependence of the electrical resistivity (ρ), Seebeck coefficient (S), and power factor ($S2/r$) of $(Ga_{1-x}In_x)_2Te_3$ (x = 0, 0.25, 0.5, 0.75, and 1).

random. It is very interesting that such nanostructures can be obtained by only melting and annealing of the samples under a certain condition. The unexpectedly low κ observed in Ga_2Te_3 is most likely due to the highly effective phonon scattering by the vacancy planes. We believe that natural nanostructured bulk Ga_2Te_3-related compounds would be ideal thermoelectric materials.

REFERENCES

1. T.M. Tritt and M.A. Subramanian, *Mater. Res. Soc. Bull.* 31, 188 (2006).
2. G.J. Snyder, M. Christensen, E. Nishibori, T. Caillat, and B. Iversen, *Nat. Mater.* 3, 458 (2004). doi:10.1038/nmat1154.
3. B.C. Sales and D. Mandrus, *Science* 272, 1325 (1996). doi:10.1126/science.272.5266.1325.
4. K. Kurosaki, A. Kosuga, H. Muta, M. Uno, and S. Yamanaka, *Appl. Phys. Lett.* 87, 061919 (2005). doi:10.1063/1.2009828.
5. L.D. Hicks and M.S. Dresselhaus, *Phys. Rev. B* 47, 12727 (1993). doi:10.1103/PhysRevB.47.12727.
6. L.D. Hicks, T.C. Harman, X. Sun, and M.S. Dresselhaus, *Phys. Rev. B* 53, R10493 (1996). doi:10.1103/PhysRevB.53.R10493.
7. M.S. Dresselhaus, G. Chen, M.Y. Tang, R.G. Yang, H. Lee, D.Z. Wang, Z.F. Ren, J.-P. Fleurial, and P. Gogna, *Adv. Mater.* 19, 1043 (2007). doi:10.1002/adma.200600527.
8. R. Venkatasubramanian, E. Siivola, T. Colpitts, and B. O'Quinn, *Nature* 413, 597 (2001). doi:10.1038/35098012.
9. T.C. Harman, P.J. Taylor, M.P. Walsh, and B.E. LaForge, *Science* 297, 2229 (2002). doi:10.1126/science.1072886.

10. K.F. Hsu, S. Loo, F. Guo, W. Chen, J.S. Dyck, C. Uher, T. Hogan, E.K. Polychroniadis, and M.G. Kanatzidis, *Science* 303, 818 (2004). doi:10.1126/science.1092963.
11. R.R. Desai, D. Lakshminarayana, P.B. Patel, P.K. Patel, and C.J. Panchal, *Mater. Chem. Phys.* 94, 308 (2005). doi:10.1016/j.matchemphys.2005.05.003.
12. M. Guymont, A. Tomas, and M. Guittard, *Philos. Mag. A* 66, 133 (1992). doi:10.1080/01418619208201518.
13. K. Kurosaki, H. Matsumoto, A. Charoenphakdee, S. Yamanaka, M. Ishimaru, and Y. Hirotsu, *Appl. Phys. Lett.* 93, 012101 (2008). doi:10.1063/1.2940591.
14. N. Teraguchi, F. Kato, M. Konagai, K. Takahashi, Y. Nakamura, and N. Otsuka, *Appl. Phys. Lett.* 59, 567 (1991). doi:10.1063/1.105388.
15. A.I. Zaslavskii and V.M. Sergeeva, *Sov. Phys. Solid State* 2, 2556 (1961).